Oncogene (2009) 28, 3360–3370

www.nature.com/onc

ORIGINAL ARTICLE

MicroRNA-330 acts as tumor suppressor and induces apoptosis of prostate cancer cells through E2F1-mediated suppression of Akt phosphorylation

K-H Lee[1], Y-L Chen[2], S-D Yeh[3], M Hsiao[4], J-T Lin[5], Y-G Goan[6,7] and P-J Lu[8]

[1]Institute of Basic Medical Sciences, National Cheng Kung University, College of Medicine, Tainan, Taiwan; [2]Institute of Oral Medicine, National Cheng Kung University, College of Medicine, Tainan, Taiwan; [3]Department of Urology, Taipei Medical University, Taipei, Taiwan; [4]Genomics Research Center, Academia Sinica, Taipei, Taiwan; [5]Division of Urology Surgery, Department of Surgery, Kaohsiung Veterans General Hospital, Kaohsiung, Taiwan; [6]Department of Surgery, Kaohsiung Veterans General Hospital, Kaohsiung, Taiwan; [7]Department of Surgery, National Yang-Ming University, Taipei, Taiwan and [8]Institute of Clinical Medicine, National Cheng Kung University, College of Medicine, Tainan, Taiwan

MicroRNAs (miRNAs) make up a novel class of gene regulators; they function as oncogenes or tumor suppressors by targeting tumor-suppressor genes or oncogenes. A recent study that analysed a large number of human cancer cell lines showed that miR-330 is a potential tumor-suppressor gene. However, the function and molecular mechanism of miR-330 in determining the aggressiveness of human prostate cancer has not been studied. Here, we show that miR-330 is significantly lower expressed in human prostate cancer cell lines than in nontumorigenic prostate epithelial cells. Bioinformatics analyses reveal a conserved target site for miR-330 in the 3′-untranslated region (UTR) of E2F1 at nucleotides 1018–1024. MiR-330 significantly suppressed the activity of a luciferase reporter containing the E2F1-3′-UTR in the cells. This activity could be abolished with the transfection of anti-miR-330 or mutated E2F1-3′-UTR. In addition, the expression level of miR-330 and E2F1 was inversely correlated in cell lines and prostate cancer specimens. After overexpressing of miR-330 in PC-3 cells, cell growth was suppressed by reducing E2F1-mediated Akt phosphorylation and thereby inducing apoptosis. Collectively, this is the first study to show that E2F1 is negatively regulated by miR-330 and also show that miR-330 induces apoptosis in prostate cancer cells through E2F1-mediated suppression of Akt phosphorylation.
Oncogene (2009) **28,** 3360–3370; doi:10.1038/onc.2009.192; published online 13 July 2009

Keywords: miR-330; E2F1; Akt; apoptosis; prostate cancer

Introduction

MicroRNAs (miRNAs) are a class of small (~19–25 nt), noncoding regulatory RNAs that regulate gene expression by complementary base pairing with the 3′-untranslated region (UTR) of target mRNAs and causing their degradation or suppressing mRNA translation, which consequently lead to a decrease in target protein levels (Hutvagner and Zamore, 2002; Ambros and Chen, 2007). Recent studies have shown the importance of miRNAs in the normal regulation of gene expression during development, cell proliferation and apoptosis (Hwang and Mendell, 2007). MiRNAs have also been shown to have critical roles in tumor biology (Calin *et al*., 2004a, b; Jovanovic and Hengartner, 2006; Kent and Mendell, 2006; Volinia *et al*., 2006), thus establishing them as a relatively new and important class of oncogenes and tumor suppressor (Esquela-Kerscher and Slack, 2006). Aberrant expression of these miRNAs has been implicated in tumor growth, carcinogenesis, angiogenesis and apoptosis.

Several recent studies have presented a global analysis of miRNAs expression in human cell lines. Gaur *et al*. (2007) examined the expression profiles of 241 human miRNAs in normal tissues and the NCI-60 panel of human tumor-derived cell lines. They identified miRNAs that were downregulated in more than one major tumor cell line cluster; these were considered likely to be tumor-suppressive miRNAs. One of these miRNAs, miR-330, seemed to behave like a potential tumor suppressor in the central nervous system-derived tumor cells. Ruike *et al*. (2008) performed a quantitative measurement of 155 types of mature human miRNAs in 16 human cell lines. They also found that the expression of miR-330 was downregulated in many cancer cell lines. Taken together, these studies supported the idea that miR-330 might be a tumor-suppressive miRNA in some cancer types.

Cancer-associated chromosomal loss also causes the inactivation of genes that do not encode proteins. Several genomic regions that encode miRNAs are commonly deleted in a variety of tumors. These genes encoded small RNAs that were involved in the posttranscriptional regulation of gene expression (John *et al*., 2004). In prostate cancer, chromosome 19q was likely to harbor genes that were associated with prostate tumor aggressiveness (Neville *et al*., 2003; Slager *et al*., 2003). Two of the classical kallikrein genes KLK3 and

Correspondence: Professor P-J Lu, Institute of Clinical Medicine, National Cheng Kung University Medical College, 138, Sheng-Li Road, Tainan 704, Taiwan.
E-mail: pjlu2190@mail.ncku.edu.tw
Received 2 December 2008; revised 2 June 2009; accepted 3 June 2009; published online 13 July 2009

KLK2 on 19q13.4 were plausible candidates for prostate cancer susceptibility; however, these two genes were not likely to be involved in tumor aggressiveness (Pal *et al*., 2007). These studies suggest that unknown tumor-suppressor genes exist on chromosome 19q that have important roles in the aggressiveness of prostate cancer. MiR-330 was located on chromosome 19q13 and it was downregulated in many cancer cell lines. In our preliminary results, we found that the expression of miR-330 was downregulated in aggressive prostate cancer cell lines and a prostate cancer specimen by miR-quantitative RT–PCR and miRNA microarray analysis, respectively. These data supported our hypothesis that miR-330 was a tumor-suppressive miRNA in prostate cancer. In this study, we aimed to determine the role of miR-330 in determining the aggressiveness of prostate cancer cells and studied the regulatory mechanism of miR-330 in prostate cancer cells.

Results

miR-330 levels inversely correlate with E2F1 protein levels in prostate cancer

To determine whether miR-330 was a putative tumor suppressor in prostate cancer, we first examined the expression levels of miR-330 in three immortalized prostatic epithelial cell lines, PZ-PHV-7, PWR-1E and RWPE-1, and four prostate cancer lines, PC-3, LNCap, 22Rv1 and DU145, by miR-quantitative RT–PCR analysis. Figure 1a shows that prostate cancer cell lines have low endogenous miR-330 levels when compared with the immortalized prostatic epithelial cell lines. The results obtained from the miRNA microarray analysis also revealed that miR-330 was downregulated in prostate cancer tumors (0.33-fold of the nontumor miR-330; Supplementary Table 1; Figure 1). These data suggest that miR-330 may target oncoproteins and act as a tumor suppressor in prostate cancer cells. The bioinformatics approach from screening the 1052 nt 3′-UTR of E2F1 to RNAhybrid software analysis, a 100% match target seed sequence for miR-330 at nts 1018–1024, was identified to have minimum free energy $\Delta G \sim -15.5$ kcal/mol that was highly conserved across seven species (Figure 1b). The E2F1 protein expression was then examined by immunoblotting analysis and our results can be concluded that the miR-330 levels were inversely correlated with E2F1 protein levels in the immortalized prostatic epithelial and prostate cancer cell lines examined (Figure 1c). PZ-HPV-7, PWR-1E and RWPE-1 with high miR-330 levels showed relatively low E2F1 protein expression (Figure 1c, lanes $1 \sim 3$), whereas PC-3, LNCap, 22Rv1 and DU145 with low miR-330 levels had relatively high E2F1 protein expression (Figure 1c, lanes $4 \sim 7$).

To investigate the inverse correlation between E2F1 protein and miR-330 *in vivo*, we examined the levels of miR-330 and E2F1 protein in 11 prostate cancer tissues and 14 prostate nontumor tissues by miR-quantitative RT–PCR and immunoblotting analyses. Supplementary Table 2 summarizes the characteristics of the clinical specimens used in the study. Figures 1d and e show the results of the miR-330 and E2F1 levels in a total of 25 clinical specimens examined. To define the high or low expression level of miR-330 and E2F1 within all 25 samples, we conducted a sensitivity analysis (Altman and Bland, 1994) using different thresholds by level incremental of 10 from 10 to 270 for miR-330, and incremental of 1 from 1 to 25 for E2F1, respectively. The best cutoff threshold value of miR-330 expression was thus identified as 90, which resulted in sensitivity and specificity of 0.64 and 0.57, respectively. An expression level of miR-330 that exceeded 90 was to be defined as a high expression, and that defined obversely as low expression. Accordingly, the statistical analysis showed a significant difference of miR-330 expression level between nontumor and tumor tissues ($P = 0.042$, by χ^2-test). Most importantly, the results of correlation analysis showed that the miR-330 level was inversely correlated with the E2F1 level in a total of 25 specimens examined by Spearman's correlation analysis (correlation coefficient $r = -0.53$; $P < 0.05$). However, there was no significant correlation between miR-330 expression levels of tumor tissues and tumor grade or other clinicopathologic characteristics because of sample size limitations. To further confirm the lower miR-330 level in prostate cancer cells with higher E2F1 expression, the three NT paired tissues were used for miR-330 and E2F1 expression examination. The tumors had lower levels of miR-330 than their adjacent nontumor tissues (Supplementary Figure 2, sample nos. 1 and 3) and had higher levels of E2F1 protein than the nontumor tissues. Together with the low miR-330 level in prostate tumor tissues, when compared with prostate tissue from benign prostatic hyperplasia (BPH) patients and the inverse correlation between miR-330 and E2F1 expression, these results indicated that high miR-330 level in normal prostatic epithelium cells may have a tumor-suppressive role through negatively regulating E2F1 expression suggesting that downregulation of miR-330 may be involved in the prostate tumorigenesis and progression.

The E2F1 3′-UTR is a target for miR-330

We next investigated whether the 3′-UTR of E2F1 was a functional target of miR-330. We cloned a reporter plasmid driven by the cytomegalovirus (CMV) basal promoter that harbored the 375 nt wild-type (WT)-3′-UTR of E2F1 at the 3′-position of the luciferase reporter gene (Figure 2a, marked as WT-3′-UTR). In a parallel experiment, the conserved targeting region UGCUUUG for miR-330 binding within nts 1018–1024 was specifically mutated (Figure 2a, marked as Mut. 3′-UTR). PC-3 cells transiently transfected with the WT-3′-UTR-reporter construct and pre-miR-330 led to a significant decrease of reporter activity when compared with the control (Figure 2b, lanes 2 and 3, $P < 0.05$). The activity of the reporter construct that carried a mutated 3′-UTR was unaffected by a simultaneous transfection with pre-miR-330 (Figure 2b, lanes 4 and 5, $P > 0.1$). These results indicated that the conserved nts 1018–1024 UGCUUUG region within the E2F1 3′-UTR was

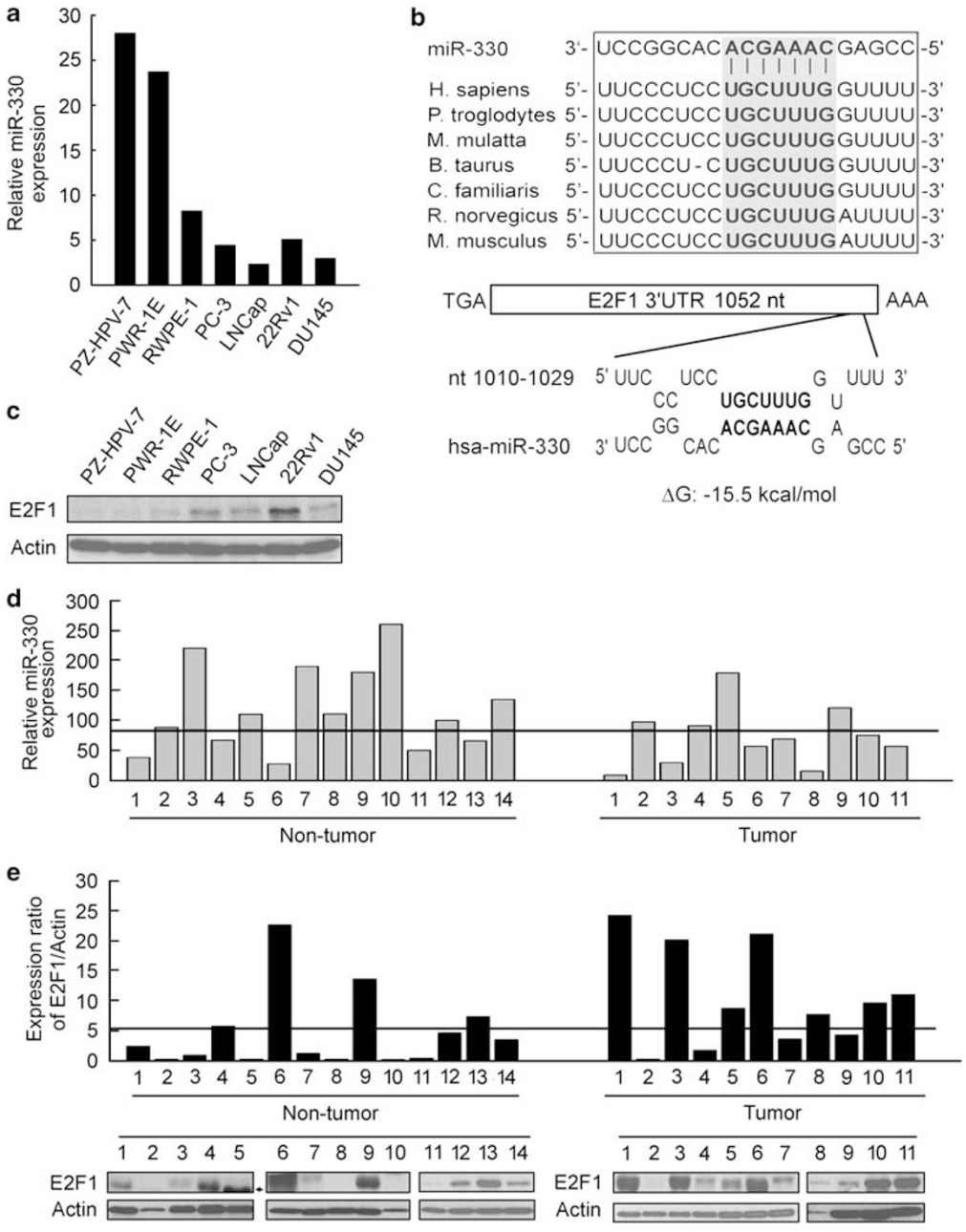

Figure 1 Inverse correlation of miR-330 and E2F1 expression levels in prostate cancer cell lines and clinical prostate tissues. (**a**) miR-quantitative RT–PCR analysis of miR-330 expression level in three immortalized prostate epithelial cell lines (PZ-HPV-7, PWR-1E and RWPE-1) and four prostate cancer cell lines (PC-3, LNCap, 22Rv1 and DU145). (**b**) The miR-330 seed-sequence and its target in seven species; its target site resides at nts 1018–1024 of the E2F1-3′-UTR. The middle seven nucleotides of miR-330 and its target region: bold; unpaired bases: above and below the duplex. (**c**) Western blotting analysis of E2F1 protein expression in seven prostate cell lines. Note that E2F1 protein levels are found high in prostate cancer cell lines and inversely correlate with miR-330 levels. (**d** and **e**) Relative miR-330 and E2F1 protein expression levels in prostate cancer specimens. Density ratio of E2F1/actin is quantified by densitometric scanning of the western blots and NIH Image J analysis (arrow indicates the nonspecific binding).

responsible for miR-330 targeting *in vitro*. To further show that miR-330 targeted on the E2F1 3′-UTR, the following experiments were carried out using an anti-miR-330. Cotransfection with anti-miR-330 and the WT-3′-UTR-reporter construct in HEK293T cells, which had a high endogenous miR-330 expression, resulted in about twofold luciferase activity increase (Figure 2c, lanes 4 and 5, $P<0.001$). Similar results were observed in PC-3 cells, which had a low level of endogenous miR-330 expression; cotransfection of anti-miR-330 and the WT-3′-UTR-reporter into PC-3 cells can cause 0.7-fold luciferase activity increase (Figure 2d, lanes 4 and 5, $P<0.01$). Taken together, these data strongly suggest that miR-330 binds to 3′-UTR of E2F1

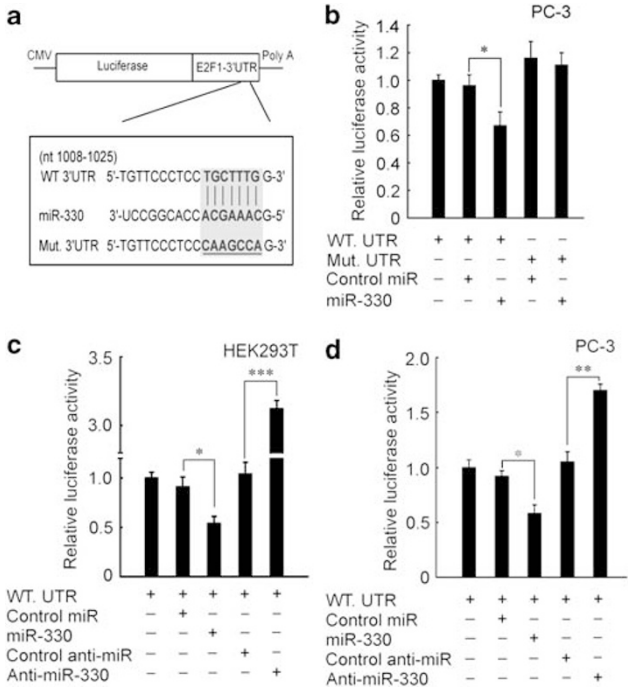

Figure 2 E2F1-3′-UTR as a target of miR-330. (**a**) Diagram of E2F1-3′-UTR-containing reporter constructs. WT represents wild type; Mut. represents mutant and contains the 7-base-mutation at the miR-330-target region that abolished binding. (**b**) Reporter assay in PC-3 cells, with the cotransfection of WT- or Mut. reporter and control-miR, or pre-miR-330 as indicated. Each bar represents the mean and s.d. of three independent experiments. (**c** and **d**) Reporter assay as in (**b**), with control anti-miR and anti-miR-330 in HEK293T and PC-3 cells, respectively. $*P<0.05$, $**P<0.01$, $***P<0.001$.

and regulates the protein levels and function of E2F1 in prostate cancer cells.

MiR-330 downregulates E2F1 and affects cell viability in prostate cancer cells

To determine whether the overexpression of miR-330 in cancer cells with low miR-330 level can decrease the E2F1 protein level and affect cell viability, PC-3, DU145 and 22Rv1 cell lines were transiently transfected with pre-miR-330 or a control-miRNA, respectively. MiR-quantitative RT–PCR and immunoblotting experiments were performed to detect the matured miR-330 level and protein levels of E2F1 and cyclin D1 (Ohtani *et al*., 1995). Compared with control miR transfection, our results showed that pre-miR-330 transfection can result in about a fourfold increase of matured miR-330 in all three prostate cancer cell lines examined (Figure 3a, lanes 1 and 2; Supplementary Figure 3). As expected, there was a significant reduction of E2F1 and cyclin D1 protein amounts in pre-miR-330-transfected but not control-miR-transfected cells (Figures 3a and b; Supplementary Figure 3). On the other hand, anti-miR-330 was used to investigate whether the downregulation of miR-330 can increase E2F1 protein level in those cancer cell lines with high endogenous miR-330 level. PZ-HPV-7 and HEK293T cell lines were then used, and transiently transfected with anti-miR-330 and followed by the miR-quantitative RT–PCR and immunoblotting analysis. Figure 3a (right panel) and Figure 3b show that anti-miR-330 transfection can downregulate the endogenous, matured miR-330 significantly (about 50% reductions in PZ-HPV-7 and HEK293T cells), and consequently lead to a significant increase in the expression of E2F1 protein and cyclin D1. The downregulation of endogenous miR-330 (33% reduction) by anti-miR-330 was also observed in PC-3 cells (Figure 3a) but only slightly affected the expression of E2F1 protein and cyclin D1 (Figure 3b). These results support our hypothesis that miR-330 binds to 3′-UTR of E2F1 and regulates the protein level of E2F1 in prostate cancer cells.

We next examined the effect of miR-330 on cell viability by using a focus formation assay. In Figure 3c, the pre-miR-330-transfected cells show low focus-forming ability, and both the size and number of the foci in pre-miR-330-transfected group are suppressed when compared with the mock or control-miR group (Figure 3c upper panel). Statistical analysis showed a significant decrease in the focus-forming ability of pre-miR-330-transfected cells (Figure 3c, bottom panel; $P<0.001$ in PC-3 and 22Rv1 cell lines, $P<0.01$ in DU145 cell line). The results of 3-(4,5-dimethylthiazol-2-yl)-2,5-diphenyltetrazolium bromide (MTT) proliferation assay further confirmed the observation above by showing that the cell proliferation index was reduced in pre-miR-330-transfected cells ($P<0.05$ in PC-3 and DU145 cell lines, $P<0.01$ in 22Rv1 cell line; Figure 3d). Interestingly, the sub-G_1-phase cell population indicating DNA fragmentation increased significantly in flow cytometric analysis when PC-3 cells were transiently transfected with pre-miR-330 (Table 1; 4.2% in control miR vs 15.4% in pre-miR-330-transfected cells, $P<0.001$). Collectively, these results suggest that miR-330 can downregulate the E2F1 protein level that negatively regulates prostate cell cell viability by causing cell apoptosis.

MiR-330 negatively regulates cell viability by inhibition of the Akt survival pathway in prostate cancer cells

Several studies have shown the importance of the Akt kinase and mitogen-activated protein kinase (MAPK) signaling pathways in regulating cell growth, survival and the inhibition of apoptosis in prostate cancer (Tyagi *et al*., 2003; Ayala *et al*., 2004; Thomas *et al*., 2004). Thus, we used a human phospho-MAPK array to monitor change in phosphorylation states in response to miR-330; this array included major MAPK families (ERK, p38 and JNK) as well as intracellular kinases, such as Akt, GSK-3β and p70 S6, which were important in signal transduction and cellular proliferation. As shown in Figures 4a and b, after 12 h pre-miR-330 transfection, miR-330 is found to significantly decrease the phosphorylation levels of intracellular kinases (Akt1, Akt2, Akt3, Akt pan, GSK-3α/β) and ERK, but not p38 and JNK examined in PC-3 cells.

To confirm this observation, immunoblotting analyses were performed to investigate whether increasing miR-330 in PC-3 cells could specifically suppress Akt

phosphorylation without affecting MAPK. As shown in Figures 4c and d, miR-330 treatment of the PC-3 cell line results in a marked reduction of phosphorylated Akt at Ser473 and Thr308 ($P<0.01$; Figure 4d). In contrast, there was no significant change in the phosphorylation levels of ERK, p38 and JNK after

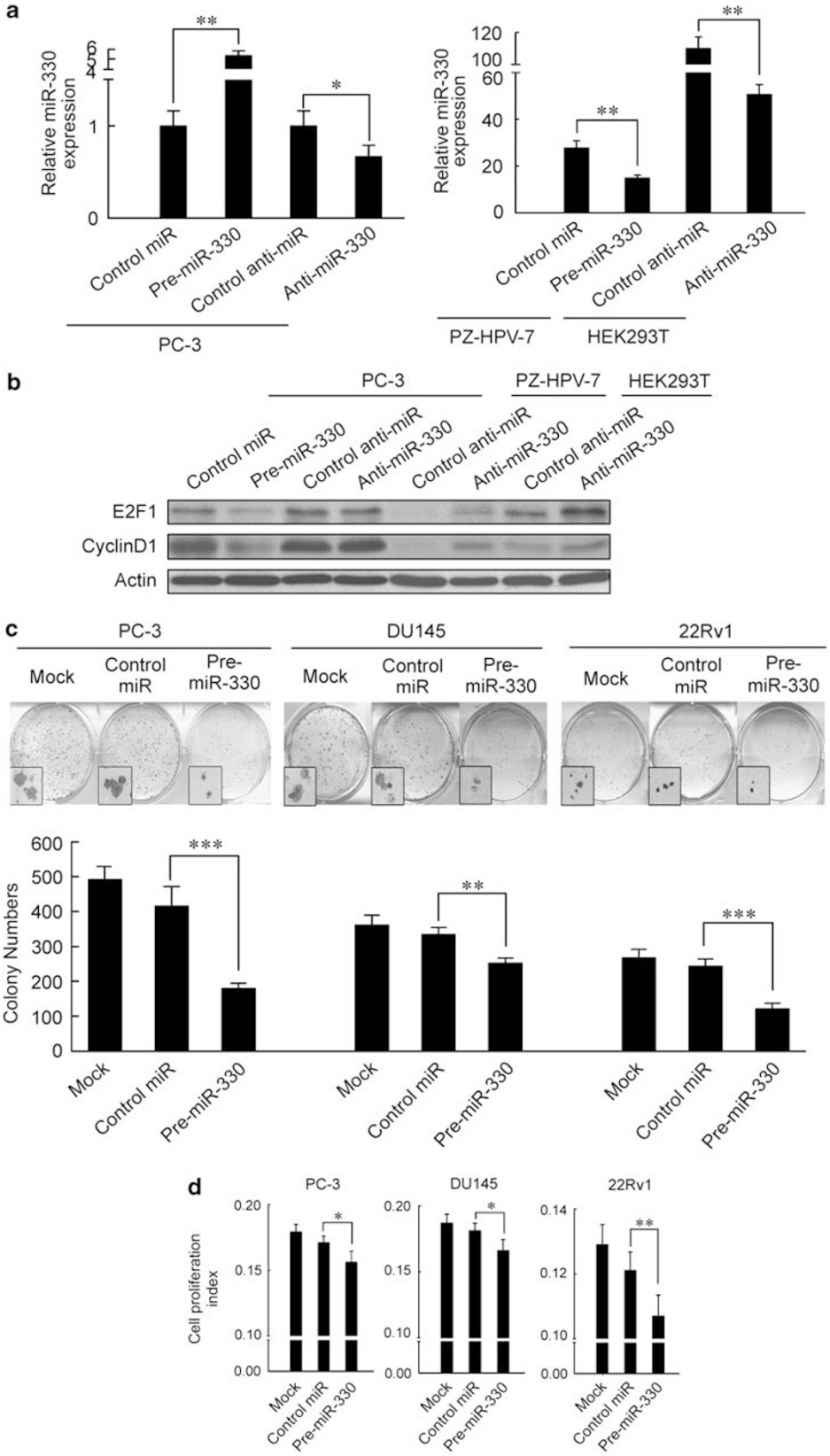

the pre-miR-330 transfection. On the basis of the above results, miR-330 induces apoptosis in prostate cancer cells by inhibiting the Akt survival pathway.

Table 1 Cell-cycle distribution of pre-miR-330-transfected PC-3 cells

Cell-cycle phase	*DNA content (%)*		
	24 h		
	Mock	*Control miR*	*Pre-miR-330*
Sub-G_1	2.1 ± 0.89	4.2 ± 1.06	15.4 ± 2.34
G_1	64.8 ± 3.36	61.6 ± 4.78	56.1 ± 3.61
S	9.6 ± 1.29	9.1 ± 1.16	4.7 ± 0.78
G_2/M	23.5 ± 2.11	25.1 ± 2.33	23.8 ± 2.12

MiR-330 induces apoptosis of PC-3 cells through E2F1-mediated suppression of Akt phosphorylation

Previous studies have revealed that Akt inhibits cell apoptosis by phosphorylating and inactivating apoptotic factors, such as Bad and caspase-9 (Datta *et al*., 1997). To show the miR-330-induced cell apoptosis through the Akt-mediated pathway, the phosphorylation level of Bad and caspase-9 were examined in pre-miR-330-transfected PC-3 cells, respectively. As shown in Figure 5a, Bad phosphorylation at Ser-136 and caspase-9 phosphorylation at Ser-196 are significantly decreased in miR-330 overexpressed PC-3 cells, in which both E2F1 protein level and Akt phosphorylation are markedly reduced. Suppression of Bad Ser-136 phos-

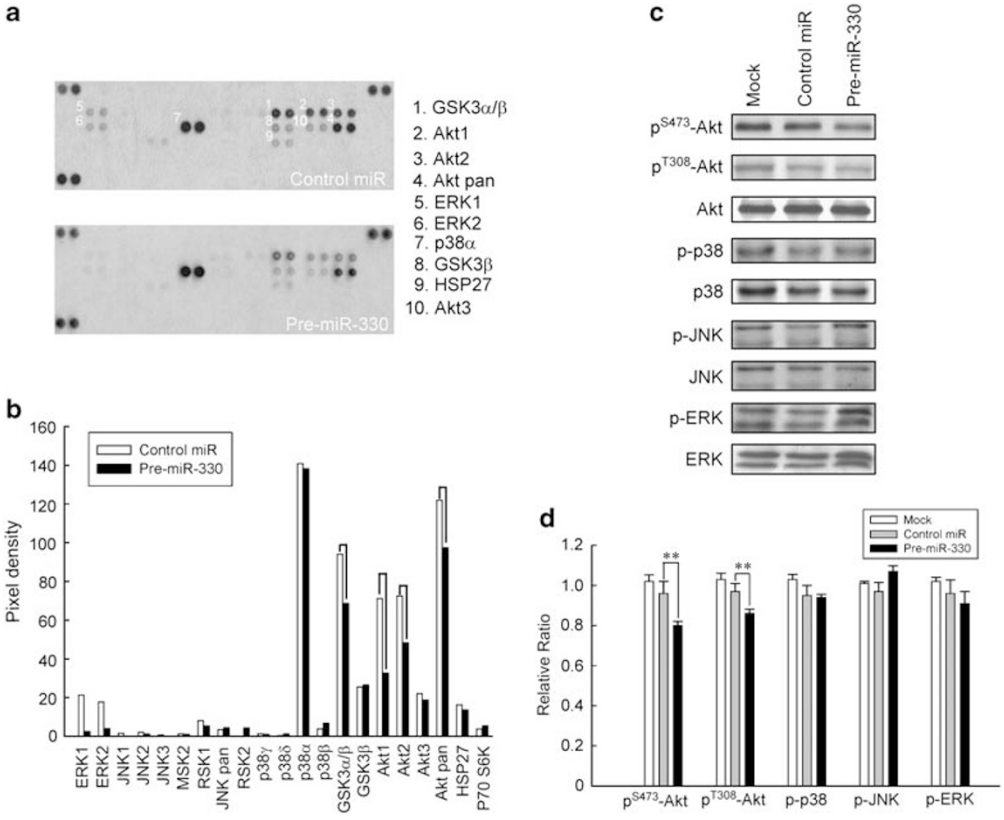

Figure 4 Detection and comparison of multiple phosphorylated kinase expression changes after transfection with pre-miR-330 or control miR by human phosphorylated mitogen-activated protein kinase (MAPK) array. (**a**) Detection of control miR/pre-miR-330-modulated intracellular kinases in PC-3 cells in dotted array. PC-3 cells are transfected with control miR or pre-miR-330. After 12 h, cells are harvested, lysed and analysed for MAPK activity as described in Materials and methods. Each phosphorylated MAPK array displays duplicate signal spots for each gene, as well as three internal positive controls and six negative controls. (**b**) Comparison of pixel density of the phosphorylated MAPK array signals. Dot density is scanned from the scanned X-ray film and the images are analysed and quantified using image analysis software (NIH-Image J). (**c**) Western blots analysis of multiple kinases after transfection with pre-miR-330 and control miR. The cell lysates obtained from the experiment described for(**a**) are separated by SDS–polyacrylamide gel electrophoresis (PAGE); the gels are immunoblotted using antibodies specific for p-S473-Akt, p-T308-Akt, Akt, p-p38, p38, p-JNK, JNK, p-ERK and ERK. (**d**) Relative expression levels of phosphorylated Akt, p38, JNK and ERK detected by western blots above (in **c**) and quantified and normalized to their total amount. $^{**}P<0.01$.

Figure 3 MiR-330 regulates E2F1 expression at the posttranscriptional level and suppresses cell proliferation. (**a** and **b**) Relative miR-330 expression and western blot analysis of E2F1 and cyclin D1 in PC-3, PZ-HPV-7 and HEK293 T cells after miR-330 or anti-miR-330 transfection as indicated. (**c**) Focus-forming assay of pre-miR-330-transfected prostate cancer cell lines. Mean values of the foci from triplicate experiments are shown in the lower panel ($^{**}P<0.01$, $^{***}P<0.001$). Bars indicate the standard deviations. (**d**) Cell proliferation analysis after pre-miR-330 transfection by 3-(4,5-dimethylthiazol-2-yl)-2,5-diphenyltetrazolium bromide (MTT) assay. The cells with control-miR or pre-miR-330 constructs are plated in 12-well culture dishes (5×10^5 cells/well). Cells growth is measured after 24 h with the MTT proliferation assay.

phorylation initiates apoptosis by binding to the antiapoptotic molecules Bcl-xL and Bcl-2 on the outer mitochondrial membrane, and causes cytochrome C release into the cytoplasm (Guo *et al*., 2007). We next investigated whether the cytochrome C was released from mitochondria on treatment of pre-miR-330. In contrast to the control group where most of the cytochrome C remained in mitochondria, a robust amount of cytochrome C was found in cytoplasm 24 h after pre-miR-330 treatment (Figure 5b). Interestingly, procaspase-3 cleavage was also detected 24 h after pre-miR-330 treatment. Figure 5c shows that increased amounts of cleaved poly-(ADP-ribose) polymerase (PARP) are in proportion to the processing of caspase-3 cleavage suggesting that miR-330-induced apoptosis in PC-3 cells is dependent on caspase-3. As the phosphorylated H2AX could be used as an indicator for DNA damage and fragmentation (Rogakou *et al*., 2000), we

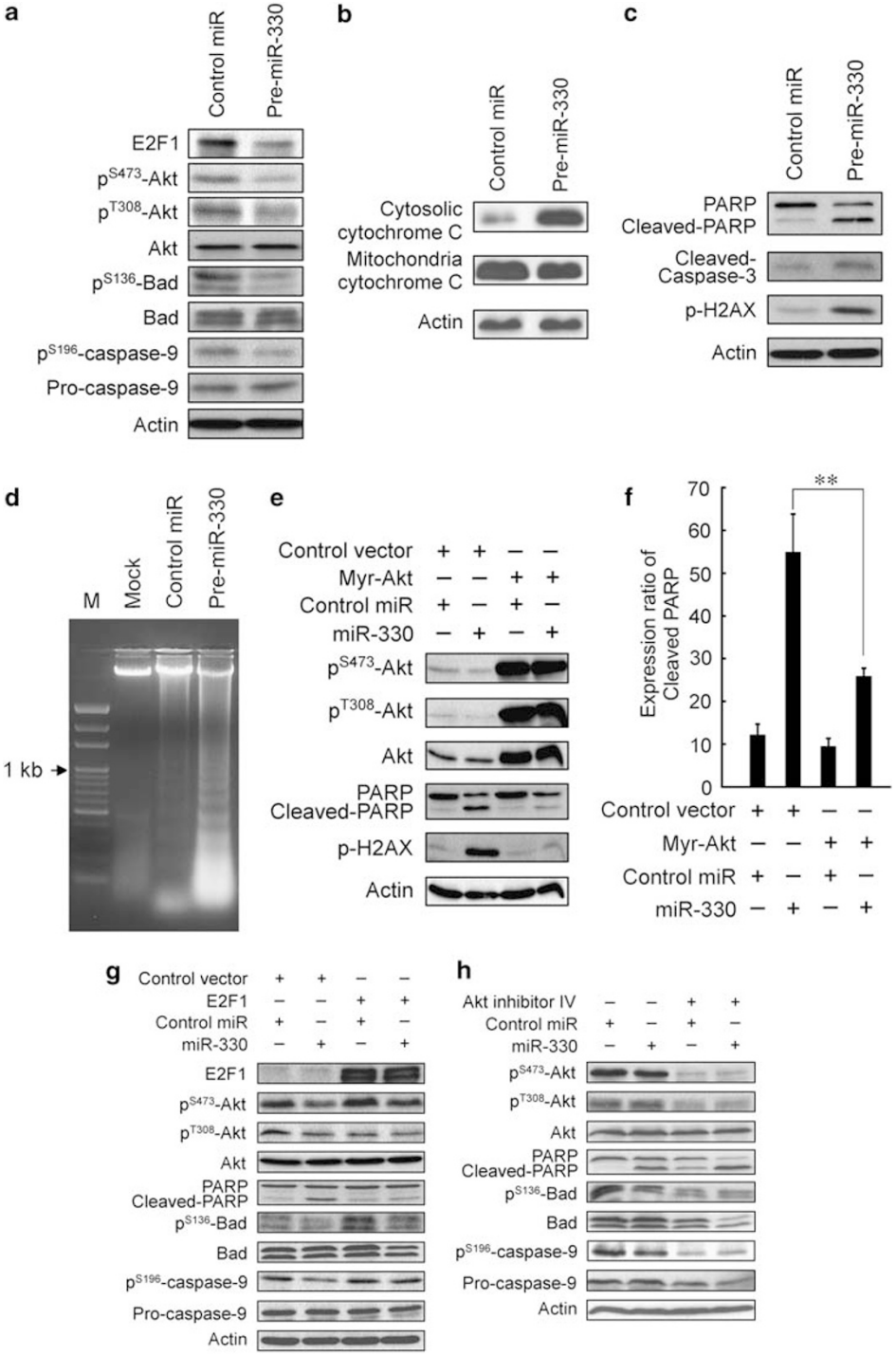

then used the phosphorylated H2AX immunoblotting and DNA laddering assay to confirm the DNA fragmentation after pre-miR-330 transfection. As shown in Figure 5c, the immunoreactivity of the phospho-H2AX level increases about twofold in pre-miR-330-transfected cells when compared with the control group. The DNA fragmentation was further confirmed by showing that ectopic pre-miR-330 expression increased the DNA laddering, but not in the control miR group (Figure 5d). Taken together, these data strongly suggested that the downregulation of Akt was involved in pre-miR-330-mediated apoptosis. Overexpression of a constitutively active Akt or overexpression of E2F1 was then hypothesized to restore the pre-miR-330-mediated apoptosis. To test this hypothesis, PC-3 cells were cotransfected with pre-miR-330 and myr-Akt, followed by the PARP cleavage and H2AX phosphorylation examination. The results revealed that myr-Akt can effectively suppress miR-330-induced PARP cleavage and H2AX phosphorylation (Figures 5e and f, lanes 2 and 4). Moreover, we investigated whether overexpression of E2F1 can inhibit miR-330-mediated apoptosis. As shown in Figure 5g, E2F1 overexpression in PC-3 cells can cause the phosphorylated level of Akt at Ser473 increase (Figure 5g, lanes 1 and 3). As expected, the decrease in the phosphorylation of Bad and caspase-9 was restored in pre-miR-330 and E2F1 cotransfected cells (Figure 5g, lanes 2 and 4). Furthermore, we also examined whether the Akt inhibitor can synergize with miR-330 in inducing apoptosis in PC-3 cells. As shown in Figure 5h, the levels of Akt phosphorylation at Ser473 and Thr308 are decreased by treatment with Akt inhibitor IV, in which the cleaved PARP is significantly increased (Figure 5h, lanes 2 and 4). Taken together, our results show that pre-miR-330 induced PC-3 apoptosis through E2F1-mediated suppression of Akt phosphorylation, and that overexpression of a constitutively active Akt or E2F1 can abolish pre-miR-330-mediated apoptosis.

Discussion

This is the first study to show that the oncogene E2F1 is negatively regulated by miR-330 at the posttranscriptional level through a specific target site (nt 1018–1024) within the 3′-UTR. We also showed that miR-330 induced apoptosis through E2F1-mediated suppression of Akt phosphorylation in prostate cancer cells. The *in vivo* relevance of these findings is supported by the data from resected tissues of prostate cancer patients, which show that high levels of miR-330 significantly correlate with low levels of E2F1 protein.

Until recently, very little experimental work had been performed to assess the effects of miRNA in prostate cancer. Three groups have investigated the expression of miRNAs in clinical prostate cancer samples using miRNA microarray analysis (Volinia *et al*., 2006; Porkka *et al*., 2007; Ozen *et al*., 2008). However, conflicting results were reported in these studies. For example, a comparison of the 12 differentially expressed miRNAs data from the results of Volinia *et al*. (2006) and Porkka *et al*. (2007) showed that only 3 miRNAs (let-7a, miR-184 and miR-198) displayed similar expression level, whereas the remaining 9 (let-7d, miR-16, miR-26a, miR-27a, miR-29a, miR-29b, miR-30c, miR-92 and miR-195) showed reverse differential expression levels. Supplementary Table 1 lists the differentially expressed miRNAs between prostate cancer tissues and their nontumor tissues obtained from our miRNA microarray experiments (Supplementary Figure 1). We found that 3 miRNAs (miR-206, miR-17-5p and miR-101-1) in a total of 10 upregulated miRNAs in prostate cancer tissue were consistent with those of Volinia *et al*. (2006). On the other hand, 2 miRNAs (let-7f-2 and let-7b) out of the 10 downregulated miRNAs in prostate cancer tissue in our results were found to be consistent with Porkka's data (Porkka *et al*., 2007). The plausible explanations for these conflicting data may be: (1) the usage of BPH tissue as a nontumor group in our study and (2) the possible contamination of prostate cancer cells with adjacent benign tissue and/or stromal cells, including fibroblasts, smooth muscle cells and endothelial cells in prostate cancer tissues.

A number of studies have clearly shown that one miRNA could control multiple genes, whereas one gene could also be regulated by multiple miRNAs (Uney and Lightman, 2006). For example, a recent study has

Figure 5 Induction of apoptosis in PC-3 cells by pre-miR-330 through E2F1-mediated suppression of Akt phosphorylation. (**a**) MiR-330 overexpressed in PC-3 cells decreases the expression of E2F1 and the phosphorylation of Akt (S473 and T308), Bad (Ser136) and caspase-9 (Ser196). (**b**) Cytosolic and mitochondria cytochrome C protein expression analysis in pre-miR-330-transfected PC-3 cells. Note that both cytosolic cytochrome C protein levels increase after pre-miR-330 transfection. (**c**) Western blot analysis of apoptosis-associated proteins poly-(ADP-ribose) polymerase (PARP), Caspase 3 and H2AX after pre-miR-330 transfection in PC-3 cells. Note that PARP is cleaved as the result of caspase 3 activation in apoptotic cells after the transfection of PC-3 cells with pre-miR-330. Also note that the phosphorylation of H2AX increases under the same conditions. (**d**) DNA ladder analysis of ectopic pre-miR-330 expression in PC-3 cells. Note that significant DNA ladders are found in miR-330-transfected cells. (**e**) Western blot analysis of Akt phosphorylation and apoptosis-associated proteins after pre-miR-300 and myr-Akt cotransfection. PC-3 Cells are transfected with control miR, pre-miR-330 with or without myr-Akt. Equal amount of cell lysates are analysed by western blot analysis. Note that inhibition of pre-miR-330 induces PARP cleavage by cotranfection with myr-Akt. (**f**) Relative expression of cleaved PARP after miR-330 and myr-Akt cotranfection. Cleaved PARP is measured by western blot results in (**e**) and quantitative analysis is performed by NIH-Image software. The results are from three independent experiments. (**g**) E2F1 overexpression restored miR-330-induced decrease of Akt, Bad and caspase-9 phosphorylation and PARP cleavage. (**h**) Western blot analysis of Akt, Bad and caspase-9 phosphorylation and apoptosis-associated protein after pre-miR-330 transfection and Akt inhibitor IV treatment. PC-3 cells are transfected with control miR or pre-miR-330. After transfection for 4 h, the Akt inhibitor IV (1 μM, dissolved in DMSO) or dimethyl sulfoxide (DMSO) is added into cells for 12 h and western blot analysis is then performed (**$P<0.01$).

revealed that miR-106b, miR-93, miR-17-5p and miR-20a, which were located on separated miRNA clusters, can cooperate to inhibit E2F1 translation (O'Donnell *et al*., 2005; Petrocca *et al*., 2008). Many evidences, including those presented in this study, supported our conclusion that E2F1 was regulated by miR-330 in prostate cancer tumorigenesis, which are listed below. First, miR-330, which was located at chromosome 19q13, has been reported to be strongly linked to the aggressiveness of prostate cancer (Slager *et al*., 2003; Pal *et al*., 2007). Second, it has been shown that E2F1 was significantly overexpressed in metastatic and hormone-resistant prostate cancer (Davis *et al*., 2006). Third, prostate cancer cells with a high level of E2F1 protein expression had low levels of endogenous miR-330 expression (Figures 1a and c). Collectively, these results showed that the expression of E2F1 was regulated by miR-330 and that the level of E2F1 protein expression was inversely correlated with miR-330 expression in prostate cancer cells.

Previously deregulated E2F1 expression can either promote or inhibit tumorigenesis depending on the nature of the other oncogenic mutations that are present (Johnson and DeGregori, 2006). It triggers both proliferation and apoptosis through activation of downstream target genes. Thus, if the pathways that mediate E2F1-induced apoptosis are disabled, E2F1 functions strictly as a growth promoter (Stanelle and Pützer, 2006). Overexpression of E2F1 was shown to be oncogenic, and predisposing cells to neoplastic transformation (Pierce *et al*., 1999). However, the major effect of E2F1 in conferring numerous survival advantages has been shown to be mediated through the activation of the Akt-signaling pathway (Chaussepied and Ginsberg, 2004; Liu *et al*., 2006). The activation of Akt was shown to be associated with the inhibition of various proapoptotic effectors and the suppression of Ask1/p38MAPK/JNK-mediated cell death (Kennedy *et al*., 1997; Zhou *et al*., 2000; Testa and Bellacosa, 2001; Tsuruta *et al*., 2002). In this study, we showed that miR-330 can significantly decrease the phosphorylation of targeted intracellular kinases (p-Akt1, p-Akt2, p-Akt3 and p-GSK-3β) in PC-3 cells (Figure 4). Among three members of the PKB/Akt, the activation of Akt-1 was required most for both cell survival and cell proliferation. Together with that, Akt-mediated survival signaling was blocked and consequently caused apoptotic signaling activation (Figure 5) in pre-miR-330 treated PC-3 cells; these results showed that miR-330 might achieve antiproliferation, at least in part, through negatively regulating E2F1 expression.

In conclusion, our study suggested that the oncogene E2F1 was negatively regulated at the posttranscriptional level by miR-330 through a specific target motif at nts 1018–1024 of the E2F1-3′-UTR. Furthermore, miR-330 induced apoptosis and antiproliferation in prostate cancer cells (Figure 6). These data, together with our data from resected patient prostate tumors, may support a strategy for targeting with the miR-330/E2F1 interaction or rescuing miR-330-expression as a new therapeutic application to treat prostate cancer patients in the future.

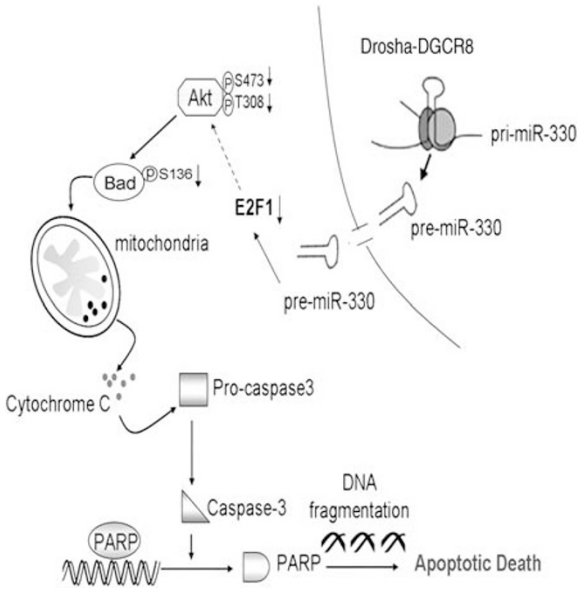

Figure 6 Model of cellular apoptosis triggered by tumor suppressor miR-330 through E2F1-Ak-mediated pathway.

Materials and methods

Cell cultures

PC-3, LNCaP and 22Rv1 cell lines (ATCC, Rockville, MD, USA) were cultured in RPMI 1640, supplemented with 10% fetal bovine serum (FBS) and antibiotics. DU145 (ATCC) cell line was cultured in Minimum Essential Eagle's medium supplemented with 10% FBS and 2 mM L-glutamine with antibiotics. PZ-HPV-7, PWR-1E and RWPE-1 (ATCC) human nontumorigenic prostate epithelial cell lines were cultured in keratinocyte serum-free medium supplemented with 0.2 ng/ml rEGF and 30 μg/ml bovine pituitary extract. Cultures were maintained in a 5% CO_2 humidified atmosphere at 37 °C.

Clinical specimens

Human prostate specimens were obtained from Kaohsiung Veterans General Hospital (Kaohsiung, Taiwan) and Taipei Medical University Hospital (Taipei, Taiwan). All patients gave informed consent and the protocol was approved by the IRB Committee before a tissue sample was collected during their planned surgery. The carcinoma samples were obtained from a palliative transurethral resection of the prostate and histologically examined for the presence of tumor tissue in hematoxylin and eosin-stained sections. The BPH samples were obtained from the transurethral resection of the prostate from patients treated for BPH. The specimens were histologically verified not to contain any prostate cancer cells. These samples were snap frozen and stored in liquid nitrogen until used.

Reagents, antibodies and expression constructs

The candidate pri-miRNA-330 of double-stranded oligonucleotides was generated for cloning into the pcDNA6.2-GW/

EmGFP vector (Invitrogen, Carlsbad, CA, USA). The plasmid was sequenced and named pcDNA6.2-GW/EmGFP/miR-330 (pre-miR-330). pcDNA6.2-GW/±EmGFP-miR-neg control plasmid (control miR) contained an insert that could be processed into mature miRNA but not to target any known vertebrate gene. The anti-miR molecules were purchased from Ambion (Austin, TX, USA). The Akt-specific inhibitor, Akt inhibitor IV, was purchased from Calbiochem (EMD Chemicals Inc., San Diego, CA, USA). Full-length E2F1 expression vector in the mammalian expression vector, pCMV-SPORT6, was purchased from Open Biosystems (Huntsville, AL, USA). The control plasmid, pCMV-SPORT6, was generated by excising the E2F1 insert through restriction digestion. Antibodies specific for cyclin D1, Akt, phospho-Akt^{Ser473}, phospho-Akt^{T308}, Bad, phospho-Bad^{Ser136}, caspase-9, PARP, caspase-3 and phospho-H2AX^{Ser139} were purchased from Cell Signaling Technology (Beverly, MA, USA). The anti-E2F1, anti-phospho-caspase-9^{Ser196}, anti-cytochrome C, anti-PI3K-p110β and anti-actin antibodies were purchased from Santa Cruz Biotechnology (Santa Cruz, CA, USA).

Construction of the 3′-UTR-luciferase plasmid and reporter assays

The E2F1 3′-UTR target site was amplified by PCR using the primers Fwd-5′-GCAAGCTTAGCTGTTCTTCTGCC-3′ and Rev-5′-GCACTAGTGTCATCAAAATATTTATTAA-3′ and cloned downstream of the luciferase gene in the pMIR-REPORT luciferase vector (Ambion). This vector was sequenced and named WT-3′-UTR. Site-directed mutagenesis of the miR-330 target-site in the E2F1-3′-UTR was carried out using the Quick-change mutagenesis kit (Stratagene, Heidelberg, Germany) and named Mut.-3′-UTR, in which WT-3′-UTR was used as a template. For reporter assays, the cells were transiently transfected with wild-type or mutant reporter plasmid and pre-miR-330 using Lipofectamine 2000 (Invitrogen). Reporter assay was performed at 36 h posttransfection using the BriteLite plus reporter gene assay system (Perkin Elmer, Shelton, CT, USA).

Quantitative RT–PCR assays for mature miRNA

The reverse transcription reactions of cell lines or human prostate cancer specimens were performed in a reaction containing 50 ng small RNA. Amplification and detection of specific products were performed with the Roche LightCycler detection system with the cycle profile according to the mirVana qRT–PCR miRNA Detection Kit (Ambion). The relative gene expression was calculated by comparing the cycle times for each target PCR. The target PCR C_t values were normalized by subtracting the internal control of 5S rRNA C_t value.

Cell viability analysis and focus formation assay

The cells were transiently transfected with control miR or pre-miR-330 plasmid DNA using Lipofectamine 2000. The effect of pre-miR-330 on the viability of cells was assessed with the MTT assay in 12 replicates according to the procedure as described previously (Shiau *et al*., 2005). For the focus formation assay, the cells seeded on 35-mm dishes at 60–80% confluence were transfected using Lipofectamine 2000 with a total of 1 μg of control miR or pre-miR-330 plasmid DNA. Twenty-four hours later, cells were trypsinized and split into six-well dishes according to the procedure as described previously (Matos *et al*., 2008).

Cell-cycle analysis and DNA fragmentation assay

PC-3 cells were transfected with control miR or pre-miR-330 plasmid DNA for 24 h and cell-cycle analysis or DNA fragmentation assay was then performed. The distribution of cell-cycle phases was assayed by propidium iodide staining and flow cytometry (FACScan; BD Biosciences, San Jose, CA, USA). DNA fragmentation analysis was performed as previously described (Kim *et al*., 1999).

Subcellular fractionation

PC-3 cells (5×10^6) were harvested with ice-cold phosphate-buffered saline. Cells were resuspended in 500 μl of buffer A (20 mM Hepes–KOH, pH 7.5, 10 mM KCl, 1.5 mM $MgCl_2$, 1 mM sodium EDTA, 1 mM sodium EGTA, 1 mM dithiothreitol) containing 250 mM sucrose and a mixture of protease inhibitors (1 mM phenylmethylsulfonyl fluoride, 1% aprotinin, 1 mM leupeptin). Subcellular fractionation was performed as previously described (Krajewski *et al*., 1993).

Human phospho-kinase array

PC-3 cells (1.2×10^6) were transfected in 10-cm plates with 5 μg of control miR or pre-miR-330 plasmid DNA. At 12 h after transfection, the total protein from whole cells was purified. Cell lysates (250 μg total proteins per array) were applied and incubated with the Human Phospho-MAPK Array Kit (R&D Systems, Minneapolis, MN, USA) according to the manufacturer's instructions. Phospho-MAPK Array data were quantified using the NIH image software analysis.

Western blot analysis

Cell lines and human prostate cancer specimens were placed in lysis buffer at 4 °C for 1 h. The protein samples were electrophoresed using 10% SDS–polyacrylamide gel electrophoresis (PAGE) and performed as previously described (Leung *et al*., 2009).

Statistical analysis

Statistical analyses were performed as recommended by an independent statistician. These included the unpaired Student's *t*-test (miR-quantitative RT–PCR, luciferase reporter assay, focus formation assay, cell proliferation and western blotting quantification). The correlation of the level of miR-330 and E2F1 was determined using Spearman's test. All statistical analyses were performed using SPSS software (SPSS Inc., Chicago, IL, USA) and all values were expressed as mean ± s.d., and statistical significance was accepted for $P<0.05$ ($^*P<0.05$, $^{**}P<0.01$, $^{***}P<0.001$).

Conflict of interest

The authors declare no conflict of interest.

Acknowledgements

We thank the grant support from National Cheng Kung University Hospital Grant (NCKUH-9701004 to P-J Lu), National Science Council (NSC 97-2311-B-006-003-MY3 to P-J Lu and NSC-98-3112-B-006-012 to Y-L Chen). We also thank Dr Chen in the Department Urology College of Pharmacy and Comprehensive Cancer Center, The Ohio State University, for his generous gifts of Akt plasmid DNA.

References

Altman DG, Bland JM. (1994). Diagnostic tests: 1. Sensitivity and specificity. *BMJ* **308**: 1552.

Ambros V, Chen X. (2007). The regulation of genes and genomes by small RNAs. *Development* **134**: 1635–1641.

Ayala G, Thompson T, Yang G, Frolov A, Li R, Scardino P *et al*. (2004). High levels of phosphorylated form of Akt-1 in prostate cancer and non-neoplastic prostate tissues are strong predictors of biochemical recurrence. *Clin Cancer Res* **10**: 6572–6578.

Calin GA, Liu CG, Sevignani C, Ferracin M, Felli N, Dumitru CD *et al*. (2004a). MicroRNA profiling reveals distinct signatures in B cell chronic lymphocytic leukemias. *Proc Natl Acad Sci USA* **101**: 11755–11760.

Calin GA, Sevignani C, Dumitru CD, Hyslop T, Noch E, Yendamuri S *et al*. (2004b). Human microRNA genes are frequently located at fragile sites and genomic regions involved in cancers. *Proc Natl Acad Sci USA* **101**: 2999–3004.

Chaussepied M, Ginsberg D. (2004). Transcriptional regulation of AKT activation by E2F. *Mol Cell* **16**: 831–837.

Datta SR, Dudek H, Tao X, Masters S, Fu H, Gotoh Y *et al*. (1997). Akt phosphorylation of BAD couples survival signals to the cell-intrinsic death machinery. *Cell* **91**: 231–241.

Davis JN, Wojno KJ, Daignault S, Hofer MD, Kuefer R, Rubin MA *et al*. (2006). Elevated E2F1 inhibits transcription of the androgen receptor in metastatic hormone-resistant prostate cancer. *Cancer Res* **66**: 11897–11906.

Esquela-Kerscher A, Slack FJ. (2006). Oncomirs-microRNAs with a role in cancer. *Nat Rev Cancer* **6**: 259–269.

Gaur A, Jewell DA, Liang Y, Ridzon D, Moore JH, Chen C *et al*. (2007). Characterization of microRNA expression levels and their biological correlates in human cancer cell lines. *Cancer Res* **67**: 2456–2468.

Guo X, Chen KH, Guo Y, Liao H, Tang J, Xiao RP. (2007). Mitofusin 2 triggers vascular smooth muscle cell apoptosis via mitochondrial death pathway. *Circ Res* **101**: 1113–1122.

Hutvagner G, Zamore PD. (2002). A microRNA in a multiple-turnover RNAi enzyme complex. *Science* **297**: 2056–2060.

Hwang HW, Mendell JT. (2007). MicroRNAs in cell proliferation, cell death, and tumorigenesis. *Br J Cancer* **96**(Suppl): R40–R44.

John B, Enright AJ, Aravin A, Tuschl T, Sander C, Marks DS. (2004). Human MicroRNA targets. *PLoS Biolo* **2**: 1862–1879.

Johnson DG, Degregori J. (2006). Putting the oncogenic and tumor suppressive activities of E2F into context. *Curr Mol Med* **6**: 731–738.

Jovanovic M, Hengartner MO. (2006). miRNAs and apoptosis: RNAs to die for. *Oncogene* **25**: 6176–6187.

Kennedy SG, Wagner AJ, Conzen SD, Jordan J, Bellacosa A, Tsichlis PN *et al*. (1997). The PI 3-kinase/Akt signaling pathway delivers an anti-apoptotic signal. *Genes Dev* **11**: 701–713.

Kent OA, Mendell JT. (2006). A small piece in the cancer puzzle: microRNAs as tumor suppressors and oncogenes. *Oncogene* **25**: 6188–6196.

Kim R, Ohi Y, Inoue H, Aogi K, Toge T. (1999). Introduction of gadd153 gene into gastric cancer cells can modulate sensitivity to anticancer agents in association with apoptosis. *Anticancer Res* **19**: 1779–1783.

Krajewski S, Tanaka S, Takayama S, Schibler M J, Fenton W, Reed JC. (1993). Investigation of the subcellular distribution of the bcl-2 oncoprotein: residence in the nuclear envelope, endoplasmic reticulum, and outer mitochondrial membranes. *Cancer Res* **53**: 4701–4714.

Leung KW, Tsai C H, Hsiao M, Tseng C J, Ger L P, Lee K H *et al*. (2009). Pin1 overexpression is associated with poor differentiation and survival in oral squamous cell carcinoma. *Oncol Rep* **21**: 1097–1104.

Liu K, Paik JC, Wang B, Lin FT, Lin WC. (2006). Regulation of TopBP1 oligomerization by Akt/PKB for cell survival. *EMBO J* **25**: 4795–4807.

Matos P, Oliveira C, Velho S, Goncalves V, da Costa LT, Moyer MP *et al*. (2008). B-Raf (V600E) cooperates with alternative spliced Rac1b to sustain colorectal cancer cell survival. *Gastroenterology* **135**: 899–906.

Neville PJ, Conti DV, Krumroy LM, Catalona WJ, Suarez BK, Witte JS *et al*. (2003). Prostate cancer aggressiveness locus on chromosome segment 19q12-q13.1 identified by linkage and allelic imbalance studies. *Genes Chromosomes Cancer* **36**: 332–339.

O'Donnell KA, Wentzel EA, Zeller KI, Dang CV, Mendell JT. (2005). c-Myc-regulated microRNAs modulate E2F1 expression. *Nature* **435**: 839–843.

Ohtani K, DeGregori J, Nevins JR. (1995). Regulation of the cyclin E gene by transcription factor E2F1. *Proc Natl Acad Sci USA* **92**: 12146–12150.

Ozen M, Creighton CJ, Ozdemir M, Ittmann M. (2008). Widespread deregulation of microRNA expression in human prostate cancer. *Oncogene* **27**: 1788–1793.

Pal P, Xi H, Sun G, Kaushal R, Meeks JJ, Thaxton CS *et al*. (2007). Tagging SNPs in the kallikrein genes 3 and 2 on 19q13 and their associations with prostate cancer in men of European origin. *Hum Genet* **122**: 251–259.

Petrocca F, Visone R, Onelli MR, Shah MH, Nicoloso MS, de Martino I *et al*. (2008). E2F1-regulated microRNAs impair TGFbeta-dependent cell-cycle arrest and apoptosis in gastric cancer. *Cancer Cell* **13**: 272–286.

Pierce AM, Schneider-Broussard R, Gimenez-Conti IB, Russell JL, Conti CJ, Johnson DG. (1999). E2F1 has both oncogenic and tumor-suppressive properties in a transgenic model. *Mol Cell Biol* **19**: 6408–6414.

Porkka KP, Pfeiffer MJ, Waltering KK, Vessella RL, Tammela TL, Visakorpi T. (2007). MicroRNA expression profiling in prostate cancer. *Cancer Res* **67**: 6130–6135.

Rogakou EP, Nieves-Neira W, Boon C, Pommier Y, Bonner WM. (2000). Initiation of DNA fragmentation during apoptosis induces phosphorylation of H2AX histone at serine 139. *J Biol Chem* **275**: 9390–9395.

Ruike Y, Ichimura A, Tsuchiya S, Shimizu K, Kunimoto R, Okuno Y *et al*. (2008). Global correlation analysis for micro-RNA and mRNA expression profiles in human cell lines. *J Hum Genet* **53**: 515–523.

Shiau CW, Yang CC, Kulp SK, Chen KF, Chen CS, Huang JW. (2005). Thiazolidenediones mediate apoptosis in prostate cancer cells in part through inhibition of Bcl-xL/Bcl-2 functions independently of PPARgamma. *Cancer Res* **65**: 1561–1569.

Slager SL, Schaid DJ, Cunningham JM, McDonnell SK, Marks AF, Peterson BJ *et al*. (2003). Confirmation of linkage of prostate cancer aggressiveness with chromosome 19q. *Am J Hum Genet* **72**: 759–762.

Stanelle J, Pützer BM. (2006). E2F1-induced apoptosis: turning killers into therapeutics. *Trends Mol Med* **12**: 177–185.

Testa JR, Bellacosa A. (2001). AKT plays a central role in tumorigenesis. *Proc Natl Acad Sci USA* **98**: 10983–10985.

Thomas GV, Horvath S, Smith BL, Crosby K, Lebel LA, Schrage M *et al*. (2004). Antibody-based profiling of the phosphoinositide 3-kinase pathway in clinical prostate cancer. *Clin Cancer Res* **10**: 8351–8356.

Tsuruta F, Masuyama N, Gotoh Y. (2002). The phosphatidylinositol 3-kinase (PI3 K)-Akt pathway suppresses Bax translocation to mitochondria. *J Biol Chem* **277**: 14040–14047.

Tyagi A, Agarwal R, Agarwal C. (2003). Grape seed extract inhibits EGF-induced and constitutively active mitogenic signaling but activates JNK in human prostate carcinoma DU145 cells: possible role in antiproliferation and apoptosis. *Oncogene* **22**: 1302–1316.

Uney JB, Lightman SL. (2006). MicroRNAs and osmotic regulation. *Proc Natl Acad Sci USA* **103**: 15278–15279.

Volinia S, Calin GA, Liu CG, Ambs S, Cimmino A, Petrocca F *et al*. (2006). A microRNA expression signature of human solid tumors defines cancer gene targets. *Proc Natl Acad Sci USA* **103**: 2257–2261.

Zhou H, Li XM, Meinkoth J, Pittman RN. (2000). Akt regulates cell survival and apoptosis at a postmitochondrial level. *J Cell Biol* **151**: 483–494.

Supplementary Information accompanies the paper on the Oncogene website (http://www.nature.com/onc)